JOINT EUROPEAN TORUS JET

JET–P(93)95

M.C. Ramos de Andrade, M. Brusati, Y. Baranov,
L-G. Eriksson, C. Gormezano, E. Righi, F. Rimini, G. Sadler

Interaction of Lower Hybrid Waves with Fast Ions in JET

Interaction of Lower Hybrid Waves with Fast Ions in JET

M.C. Ramos de Andrade[1], M. Brusati, Y. Baranov,
L-G. Eriksson, C. Gormezano, E. Righi[2], F. Rimini, G. Sadler

JET-Joint Undertaking, Culham Science Centre, OX14 3DB, Abingdon, UK

[1]*Instituto de Física da Universidade ds São Paulo, São Paulo-SP, Brazil.*
[2]*Imperial College of Science, Technology and Medicine, London, SW7 2BZ, UK.*

Preprint of a paper to be submitted for publication in
Plasma Physics and Controlled Fusion
October 1993

ABSTRACT

Different diagnostic information has been employed in JET to identify the level of interaction between Lower Hybrid waves and fast ions accelerated up to few MeV by Ion Cyclotron waves. It is found that up to 25% of the Lower Hybrid power can be absorbed by fast ions under specific plasma conditions. Fourier analysis of neutron emission rates and fast ion energy signals during Lower Hybrid modulation experiments show that the level of interaction depends on the relative position of the cyclotron resonance and the Lower Hybrid absorption layers.

I–INTRODUCTION

Lower Hybrid waves (LH) have been successfully employed in tokamaks to generate plasma current by transferring momentum to the electrons in the direction parallel to the magnetic field through Electron Landau Damping (ELD). This scenario is a possible route to achieve steady-state operation in a reactor regime [1]. Lower Hybrid Current Drive (LHCD) experiments have also been performed with the objective of controlling the plasma current profile in order to stabilise MHD instabilities such as sawteeth, responsible for abrupt loss of confinement from the plasma core (disruptions).

There are however some features which have to be considered carefully in order to achieve high current drive efficiencies by using LH waves. The high density foreseen in a reactor plays an important role in limiting wave accessibility to the plasma centre, while high temperature can lead to strong electron Landau Damping at the periphery. Furthermore, high density can lead to mode conversion of the wave to the hot ion mode [2], which implies the damping of the wave on thermal ions, rather than on the electron population. This is however unlikely to occur for $n_{\|}$ spectrum produced for Lower Hybrid Current Drive (LHCD). Here $n_{\|}$ is the parallel refractive index of the wave.

It is also predicted by theory that in a reactor scenario LHCD efficiency can be affected by the damping of the wave on the 3.5MeV α particles [3, 4, 5, 6] produced during fusion reactions, since they are considered as unmagnetized $\left(k_{\perp}\rho_i << 1\right)$ [7]. This interaction occurs through perpendicular Landau damping and it affects all particles with velocities $v > \omega / k_{\perp} = c / n_{\perp}$ and which satisfy the resonance condition $v_{\perp} > \omega / k_{\perp}$. Here v and $v_{\perp}$ are respectively the module and the

perpendicular component of the α-particle velocity, $k_\perp$ and $n_\perp$ are the perpendicular components of the wave vector and the wave refractive index and $\omega/2\pi$ is the wave frequency. There are indications that at frequencies higher than 5GHz the absorption of LH power by α-particles would be negligible [8]. However, in the present state of LH technology 5 to 6GHz appears to be the highest operating frequency of an LHCD system to be considered in reactor applications. The working frequency in JET is 3.7GHz, and it is interesting to study the absorption level of LH power by ICRH driven minority ions (from now on referred to as fast ions) to try to simulate the predicted interaction of LH with α-particles in a reactor device. The interaction between LH waves and α-particles has been also simulated with neutral beam ions of a few keV of energy [8] or even 3MeV protons generated from D-D reactions [9].

The interaction of LH waves with keV hydrogen ions produced during neutral beam injection has been observed in JT-60 and the dependence of LH power absorption on the wave frequency and on the beam energy has been analysed [8]. In these experiments a critical electron density was estimated from the wave dispersion relation in order to provide the limit for which the absorption of LH power takes place for electrons or ions alternatively. Some experiments were recently performed in JT-60 using deuterium beams to analyse the mass dependence of the critical electron density mentioned above [10]. Moreover, the absorption of LH waves by D-D fusion protons has been recently observed in Tore Supra [9]. In this experiment the spectrum of thermonuclear protons has been analysed and peaks between 2 and 5MeV have been observed. The position of these peaks changes with plasma current and toroidal field values and the number of protons with energy higher than 3MeV increases almost linearly with LH injected power but decreases with electron density due to their faster slowing-down.

The first experimental evidence of the interaction of LH waves with ICRH minority ions of few MeV of energy is presented in this work. This interaction was detected in JET through measurements of the fast ion energy, γ ray and neutron emission rates and by means of Fast Fourier Transform (FFT) analysis in experiments with 100% LH power modulation.

The paper is organised in the following way: in section II the model used to describe the LH-fast ion interaction is presented. This model has been employed to build a 1-D Fokker-Planck code [11] where the competition of LH wave

damping by fast ions and fast electrons is described through an LH diffusion coefficient. In section III the diagnostic information which was used to detect the fast ion absorption of LH power is briefly described. The experimental results are described in section IV and discussed in section V. Conclusions follow in section VI.

II–THEORETICAL BACKGROUND

A theoretical model has been developed [11] to study the LH-fast ion interaction which estimates the LH power damped on the ICRH driven minority ion population as a function of plasma and wave propagation parameters. A 1-D Fokker-Planck equation in velocity space including the quasi-linear diffusion coefficients due to ICRH (D_{IC}) and LH (D_{LH}) is solved to compute the fast ion distribution function (f_{mi}) and to describe the slowing down process over a Maxwellian plasma. It is derived using the method developed by Stix to describe minority ions heated by ICRH at the fundamental harmonic [12] and consists of expanding f_{mi} in Legendre polynomials in the variable $\mu = v_{||}/v$. Zero order averaging over μ and neglecting coupling to higher order terms leads to [11]:

$$\frac{\partial f_o}{\partial t} = \frac{1}{\tau_s v^2}\frac{\partial}{\partial v}\left[\frac{T_i}{m_i v}\left(v_c^3 + \frac{T_e}{T_i}v^3\right)\frac{\partial f_o}{\partial v} + \left(v_c^3 + v^3\right)f_o + v^2\tau_s\left(D_{IC} + D_{LH}\right)\frac{\partial f_o}{\partial v}\right] \quad (2.1)$$

where f_o is the isotropic distribution function $f_o(v) = 1/2\int_{-1}^{+1} f_{mi}(\mu, v)\, d\mu$ and τ_s and v_c are respectively the slowing down time of the minority ions over a Maxwellian plasma and the critical velocity which is defined when the collision frequencies between fast ions and the bulk electron or ion populations are the same. The last two terms in eq. (2.1) describe the Quasi-Linear (QL) diffusion process in velocity space due to ICRH and LH leading to the tail formation of a given distribution function under the action of both waves. The subscript (mi) refers to the fast (minority) ions.

The ICRH diffusion coefficient can be related to the absorbed ICRH power as [12]:

$$D_{IC} = \frac{P_{abs}^{IC}}{3\ m_{mi}\ n_{mi}} \quad (2.2)$$

where m_{mi} and n_{mi} are the mass and density of the fast minority ions respectively and $P_{abs}^{IC} = P_{IC}(r)/V$ is the IC power P_{IC} coupled to the plasma per unit volume assuming a gaussian deposition profile. Since the minority heating increases preferentially the perpendicular velocity of the minority ions, these become trapped in banana orbits, in particular when the minority concentration is low or high IC power density is deposited in the plasma. When orbit effects are important, the fast ion energy is damped more effectively since fast ions reach plasma regions with lower electron temperature where slowing down is faster [13]. These effects can enlarge the region of overlapping between LH and ICRH deposition profiles. In this model these effects can be accounted for by taking broader deposition profiles for the ion cyclotron waves.

This simplified model developed by Barbato [11] to describe the interaction between LH waves and fast ions is based on the following main assumptions:

a) The QL diffusion coefficient due to LH is given by:

$$D_{LH} = \frac{\pi\ Z_{mi}^2\ e^2\ c^3}{4\ m_{mi}^2\ \omega\ v^3} \int dn_{||} \frac{\left|E(n_{||})\right|^2}{n_{\perp}^3} U\left(1 - \frac{c^2}{n_{\perp}^2 v^2}\right) \qquad (2.3)$$

where $n_{||}$ is the parallel refractive index related to $n_{\perp}$ through the wave dispersion relation and $\left|E(n_{||})\right|^2$ is the wave energy spectrum. U is the step function that indicated that only ions with $v > c/n_{\perp}$ can interact with LH waves.

b) The propagation of the wave is considered in a cylindrical geometry rather than in an elongated toroidal plasma. This means that the $n_{||}$ spectrum remains constant during the wave propagation. No ray-tracing calculations are used to describe the broadening of the $n_{||}$ spectrum. Only first pass absorption is considered and the full warm electromagnetic dispersion relation is taken into account.

When stationary solutions in the high velocity limit ($v > v_c$) are considered, eq. (2.1) is easily integrated to give:

$$f_o(v) = f_o(v_1)\ e^{-\int_{v_1}^{v} \frac{v\ dv}{\tau_s (D_{IC} + D_{LH})}} \qquad (2.4)$$

where v_1 is the lowest velocity considered in the integral. We note that when $D_{LH} = 0$, namely, outside the range where the resonance condition applies, eq. (2.4) reduces to the Stix Maxwellian solution with temperature $T_{IC} = \tau_s m_{mi} D_{IC}$. When $D_{LH} \neq 0$ a larger temperature $T = T_{IC} + T_{LH}$, where $T_{LH} = \tau_s m_{mi} D_{LH}$, characterises the fast ion distribution function. In this model the LH penetration in the plasma depends on the electron density n_e, $n_{\|}$, T_e, and P_{LH} as the deposition of the wave on the fast electron population depends on these parameters. The LH power is assumed to be launched into the plasma according to a Gaussian spectrum centred at $n_{\|_0}$ and with width $d n_{\|}$.

c) In the linear approximation, the LH power density absorbed by fast ions can be written as [11]:

$$P_{abs}^{LH} = \frac{\omega_{pmi}^2}{4\pi^{1/2}\omega} |E_{rms}|^2 \left(\frac{E_{res}}{T_{IC}}\right)^{3/2} \exp -\left(\frac{E_{res}}{T_{IC}}\right) \qquad (2.5)$$

where $|E_{rms}|^2$ is the square of the average electric field, ω_{pmi} is the plasma frequency for the fast ions and E_{res} is their resonant energy, $E_{res} = 1/2\ m_{mi}(c/n_{\perp})^2$. The dependence of the LH power absorption by fast ions on the ratio E_{res}/T_{IC} leads to a maximum P_{abs}^{LH} for $(E_{res}/T_{IC}) = 3/2$ when ICRH and LH deposition profiles are superimposed. Note that $P_{abs}^{LH} = 0$ is the limiting value when $T_{IC} \rightarrow 0$. T_{IC} is affected both by ICRH power and minority concentration even if the dependence on the latter is weak, up to 10%.

The simulations carried out with this model show that a large variation on the absorbed LH power due to a change in T_{IC} is found for peripheral wave deposition which occurs either due to high bulk temperature effects or for high $n_{\|}$ values. In this case $T_{IC}(r)$ is lower, and $E_{res}/T_{IC} >> 1$, giving a low LH power absorption by the fast ion population according to eq. (2.5). When TIC is increased, for instance by increasing the ICRH input power at a constant minority concentration, a higher absorption of the LH power is expected on this peripheral region as $E_{res}/T_{IC} \sim 1$.

Code simulations based on this model showed that LH power absorption by fast ions is found in the range of 10 to 20% in JET for electron temperatures

ranging from 5 to 7 keV, central densities between 2.5 and 3.5 $10^{19}m^{-3}$ and toroidal magnetic fields between 3 and 3.2T. Higher electron temperatures would lead to stronger electron Landau damping and the absorption by the fast ions would decrease.

III–RELEVANT MEASUREMENTS

The observation of LH wave absorption by fast ions was mainly based on the analysis of the fast ion energy, and on γ ray and neutron emission rates.

Fast Ion Energy: The fast ion energy content (W_f), is related to the anisotropic high energy tail generated during ICRF heating, which increases preferentially the perpendicular velocity component of the fast ions. Pitch angle scattering and variation of the magnetic field along the particle orbit can increase their parallel energy above the thermal level.

Two measurements of the plasma energy content on JET place different weights on the parallel and perpendicular energy of the plasma ($W_{\parallel}$ and $W_{\perp}$) and can be used to deduce the fast ion energy. These are the diamagnetic energy $W_{DIA} = \frac{3}{2}W_{\perp}$, measured by the diamagnetic loop, and $W_{MHD} = \frac{3}{4}(W_{\perp} + 2W_{\parallel})$, obtained from the fast equilibrium solver.

The fast electron contribution to the parallel plasma energy has been neglected, since it amounts to less than 1% of the bulk energy content in JET [14].

From the total energy content in the plasma:

$$W_{TOT} = W_{\perp b} + W_f + W_{\parallel}, \tag{3.1}$$

where $W_{\perp b}$ is the perpendicular energy of the plasma bulk, W_f is the fast ion energy and $W_{\parallel}$ is the total parallel energy, and taking into account that $W_{\perp b}=2\,W_{\parallel}$ (isotropic part of the distribution function), we conclude that:

$$W_f = W_{\perp} - 2W_{\parallel}, \tag{3.2}$$

with $W_{\perp} = W_{\perp b} + W_f$. We define the fast ion energy (W_f) as the perpendicular energy in excess of the isotropic component [15]. From the expressions for W_{DIA} e W_{MHD} and from eq. (3.2), we obtain W_f in terms of the plasma energy content:

$$W_f = \frac{4}{3}(W_{DIA} - W_{MHD}). \quad (3.3)$$

A relative calibration between W_{DIA} and W_{MHD} is carried out in the data analysis to ensure that $W_f = 0$ for an isotropic distribution in absence of fast ion tails.

Care has to be taken in the interpretation of W_f in sawtoothing discharges. Sawtooth crashes can be responsible for rapid changes in the energy content of fast ions due to their expulsion from the plasma centre to regions outside the q=1 surface. These ions collide with colder electrons and they slow down much faster than when they are confined in the plasma core. This leads to a fast reduction of their energy content. Simulations which assume that up to 40% of the fast ion population is expelled from the plasma centre compare well with the observed drop in the fast ion energy content [16]. We have used data that do not show rapid changes in the fast ion energy due to a sawtooth crash.

γ Rays and Neutron Emission Rate (RNT): The unstable products originating from the reactions between fast ions and the impurity ions in the plasma emit γ rays that can diagnose many aspects of the fast ion population through the analysis of the spectrum and emission rate of these rays [17]. These reactions occur in the plasma even if the density of impurities is low since the cross-sections involved in these processes are large. Impurity ions in JET plasmas consist mainly of ^{12}C and ^{9}Be. In the case of H minority heating the excitation mechanisms responsible for γ emission are respectively the inelastic scattering in the case of ^{12}C and nuclear reactions with ^{9}Be. The fast ion energy threshold in order to excite the first excited state in ^{12}C is 5MeV and approximately 1.5MeV for reactions with ^{9}Be leading to the 3.5MeV level in ^{6}Li. The associated γ line energies are 4.4 and 3.5MeV for ^{12}C and ^{9}Be respectively.

When LH waves are launched in the plasma in conjunction with ICRH waves an increase of the γ ray emission is observed after LH is switched on and these results are reported in the next section.

The neutron emission rate, mostly due to D(D, n)^{3}He reactions, also increases when LH is applied in conjunction with ICRH heating. An increase of this rate is associated with higher deuterons energy, either due to direct coupling of LH deuterons or to deuteron heating through bulk electron-ion coupling.

IV-EXPERIMENTAL RESULTS

LHCD experiments in JET were optimised for full current drive by improving the accessibility of the wave to the plasma core, optimising its coupling to the fast electron population aiming at maximising LHCD efficiency [18]. The experiments were performed in plasmas with 1 to 2MW of LH power, toroidal fields B_T = 2.6 to 3.3T, 2 and 3MA of plasma current and central density $n_e(0)$ up to 3 x $10^{19}m^{-3}$ in limiter plasmas. Hydrogen minority heating with minority concentration ranging from 5 to 15% in deuterium and helium plasmas was performed using 4 to 6MW of ICRH power with the position of the cyclotron resonance layer ranging between the plasma centre and r = 0.4m. Central electron temperatures were ranging from 5 to 8KeV. Between 1 to 2MW of LH power at 3.7GHz were launched with a power spectrum centred at a parallel refractive index $n_{\parallel}$ = 1.8 and with a Full Width Half Maximum (FWHM)=0.4. Ray tracing simulations of these plasmas show that LH wave propagation leads to $n_{\perp}$ values in the range of 10 to 25. In this case, the fast ion resonance energy E_{fi}=0.5 m_i $(c/n_{\perp})^2$ ranges from 0.75 to 4.7MeV.

The experimental results are presented as follows:

IV-i) Medium Density Pulse with 3.5MeV γ Ray Emission:

The time dependence of plasma parameters for a typical JET pulse (#27760) where LH coupling to the fast ions was observed is shown in Fig. 1. H minority heating in $^4_2$He plasmas ((H) $^4_2$He) was the heating scheme used in this case. Fig. 1d shows a total increase of 25% in the fast ion energy content, corresponding to 200kJ, when 2MW of LH power were applied in addition to 3MW of ICRH at 48MHz. Time dependent calculations carried out for this pulse to simulate the evolution of the fast ion energy according to the equation:

$$\frac{dW_f}{dt} = P_{IC} + C \times P_{LH} - \frac{2W_f}{\langle \tau_s \rangle} \qquad (4.1)$$

show that 20% of LH power has to be assumed to be absorbed by the ions in order to simulate the experimental data. In eq. (4.1) P_{IC} and P_{LH} are the ICRH and LH powers and $\langle \tau_s \rangle$ is the slowing-down time averaged over the ICRH

deposition profile. The factor C accounts for the fraction of LH power damped on the fast ions. When only ICRH power is considered in this calculation (C = 0) there is agreement between the simulated fast ion energy content and the experimental value up to 8.5s (Fig. 2). At 8.5s LH is switched on and the simulated curve does not reproduce the experimental data any longer. Although there is a step in the fast ion energy due to the density drop which takes place before 8.5s, it is observed that in order to reproduce the experimental data, 20% of LH power has to be taken into account resulting in a real increase of 140kJ (18%) in the fast ion energy. Analysis on the γ ray count rate shows an increase of more than a factor 3 after 8.5s when LH is switched on (Fig. 3). The higher emission of 3.5MeV γ rays produced from reactions between 1.5MeV ions with ^{9}Be, according to what was discussed in section III, shows an increase in the number of these ions after LH is switched on. The electron temperature measured by the LIDAR diagnostics remains constant and the observed higher γ ray rate cannot be accounted for by an increase in Z_{eff}, which remains approximately constant at 3.8. It is concluded that the cause of the higher γ count rate is the increase of the fast ion population above the 1.5MeV threshold when LH is launched in the plasma in conjunction with ICRH. The neutron emission rate also increases after 8.5s, which can be related to the more efficient heating of deuterons when LH is applied either by the direct coupling of LH to deuterium ions or by their higher energy transfer rate to bulk electrons. This increases the rate of D-D reactions and the neutron rate since these neutrons come from D-D reactions (Fig. 1e).

IV-ii) Low Density Pulse with 4.4MeV γ Ray Emission:

The plasma parameters for #27745 are shown in Fig. 4. This is a low density plasma ($n_e(0)=2.0 \times 10^{19} m^{-3}$) with a central electron temperature $T_e(0) \sim 8$keV. The ICRH heating scheme is (H) D. Fig. 5 shows the behaviour of the fast ion energy for this pulse. In this case the fast ion energy increases monotonically after 8s, when LH is switched on. The same simulations described previously for #27760 were carried out for this pulse and 30% of LH power had to be included in the fast ion power balance in order to reproduce the experimental measurements (Fig. 6). Simulations which take into account the presence of ICRH only and include fast ion orbit effects [19] show good agreement between the experimental fast ion energy and the calculated one when LH is not present. When LH is also applied, the simulated values are lower than

those deduced from experimental measurements (Fig. 7). The ICRH power deposition profiles over the thermal electron and ion populations taking into account orbit effects are shown in Fig. 8. The ion cyclotron resonance layer for this pulse is located at $r \simeq 0.15$m but orbit effects broaden the ICRH deposition profile which peaks at $r \simeq 0.35$m and extends up to approximately 0.8m, according to what is shown in Fig. 8. This gives approximately the extension where the fast ions are located in the plasma. Simulations of the LH power damped on fast ions [20], taking into account a Gaussian distribution for the minority ions centred at $r \simeq 0.15$m with a width of 0.65m show approximately 25% LH power absorption by the fast ions in agreement with the data shown in Fig. 6. Due to the low density in this case, a very high energy tail develops as indicated by the γ ray emission. The 4.4MeV γ rays produced from the scattering of fast protons on C^{12} show a substantial increase after 8s when LH is applied on top of ICRH while the 3.5MeV γ rays produced from reactions between fast ions and ^{9}Be are constant (Fig. 9). This indicates an increase in the fast ion population above 5MeV since Z_{eff} remains approximately constant. Ray tracing calculations show that for LH rays with $n_{\parallel} = 1.8$, $n_{\perp}$ values are around 10, corresponding to approximately 4.7MeV resonance energy for the fast ions (Fig. 10). The monotonic increase of D-D neutron rate after 8s, agrees with the monotonic increase of the fast ion energy content for this pulse showing that most likely deuterons have been heated more efficiently after LH is switched on either by direct coupling of the wave on the second harmonic of deuterium or by the thermalisation of the bulk electron population (Fig. 4e).

IV-iii) Comparison Between Pulses with ICRH Only and the Combined Effect with LH:

Fig. 11 shows the plasma parameters for pulses #27733 (ICRH only) and #27740 (LH and ICRH). The plasma parameters and C^{12} and Be^{9} impurity content are very similar in both cases. The 3.5MeV γ ray emission indicated that the fast ion population above 1.5MeV has a 30% higher increase with LH (#27740) when compared to the case with ICRH only (#27733), while the slow increase in both cases is explained by changes in the slowing down time associated with temperature and density behaviour (Fig. 12). The density for #27733 is slightly lower than for #27740 and the ICRH power is exactly the same for both pulses. The central electron temperature as measured by ECE shows a 10% higher value for #27740, including non thermal contribution

from the downshifted third harmonic emission. When an approximated cross-section curve for the ^{9}Be (p, a)^{6}Li reaction and typical proton energies of 1.5MeV are considered, less than 10% of the increase in the γ ray emission could be accounted for by temperature effects. This indicates that the higher increase in the γ ray rate for pulse #27740 is related to the increase of the fast ion energy content after LH is switched on. This is confirmed by the neutron emission rate increase for #27740 when LH is switched on (Fig. 11f).

IV-iv) LH Modulated Power Experiments and Localisation of ICRH Fast Minority Ions:

Finally we show results obtained by modulating the LH power. Fourier analysis (FFT) of LH power and fast ion signals in pulses with 100% LH power modulation at 1Hz was carried out for pulses #24898 and #24909. Fig. 13 shows the main plasma parameters and the IC and LH power waveforms for both pulses. Here again all the main plasma parameters are very similar. The ion cyclotron resonance layer however is different in the two pulses since the toroidal field was 2.6 and 2.9T respectively for pulses #24898 and #24909. In the first case the hydrogen minority cyclotron layer is at r = 0.4m inboard, outside the q = 1 surface, and in the second case at r = 0.1m. The Bremsstrahlung emissivity, as deduced from the Fast Electron Bremsstrahlung camera [21], shows hollow profiles peaked at r $\simeq$ 0.65m for both pulses (Figs. 14 and 15). This indicated a stronger overlap between LH and ICRH deposition profiles for pulse #24898. The FFT analysis shows a peak in the Fourier spectrum of the fast ion energy for #24898 around 1Hz, the LH modulation frequency (Fig. 16a) whereas there is no evident peak for #24909 (Fig. 16b). Peaks in higher harmonics also follow the LH Fourier spectrum in #24898.

Fig. 17 shows the neutron emission rate for both pulses. For pulse #24898 the neutron rate is modulated following the LH power modulation. This is not observed for pulse #24909. FFT analysis carried out for the neutron rate signal shows a clear peak around 1Hz for pulse #24898 (Fig. 18a), which is not present for #24909 (Fig. 18b).

These results confirm that coupling of LH waves on the fast ion population is actually taking place for pulse #24898 since nothing is observed in the

different experimental conditions for #24909 when ICRH and LH deposition profiles are not strongly overlapped.

V-DISCUSSIONS

The estimated LH power damped on the minority ions (between 20 to 30% in the cases analysed) accounts for an uncertainty of approximately 10% related to uncertainties in the measurement of the fast ion energy content W_f. The contribution of the fast electron energy content to the total parallel energy in the plasma is estimated to be in the order of 1% in JET even for a case of full current drive and very high parallel tail temperature (800keV). That allows the calculation of the fast ion energy through eq. (3.3). An off-set between with W_{DIA} and W_{MHD} energy measurement is taken into account since W_f must be zero in the absence of fast ion tails, as discussed in section III.

Possible changes in the slowing down time due to temperature or density behaviour do not explain the total increase of the fast minority energy content in presence of LH. Furthermore, plasma energy confinement times are always shorter than typical slowing down times for all analysed cases, which ensures that the estimated LH power damped on the ICRH driven ions as obtained from eq. (4.1) has not been underestimated. No absorption by neutral beam ions is observed in JET since the energies involved in this case are too low (80 or 140keV) to be resonant with the wave.

FFT analysis performed for pulses #24898 and #24909 confirmed a higher absorption of the LH waves for cases of better overlap of the LH deposition profile, deduced from FEB measurements, and the ICRH deposition profile. It is interesting to note that when the two deposition profiles overlap at larger minor radii, the damping of the wave on the fast ions is higher since the lower electron temperature decreases the efficiency of the competing fast electron absorption.

The fraction of LH power damped on the fast minority ions depends also on the minority species. Due to the mass dependence of E_{res} and to the dependence of T_{IC} on the slowing down time τ_s, E_{res}/T_{IC} is four times larger for $^3_2$He than for H, for instance. We would expect then a lower LH absorption by $^3_2$He minority ions for the same plasma conditions. Most JET discharges during LH experiments were performed with H minority ICRH heating. However, if results obtained

with ~1MeV protons at $n_\perp$ of the order of 10 to 20 are extrapolated to a case with α particles, a comparable damping rate is expected at $n_\perp \simeq 5$ to 10.

Orbit effects can spread the location fo the minority ions in the plasma thus changing the original extension of the overlapping between LH and ICRH deposition profiles. These effects might become important in the case of α-particles with large orbit widths thus increasing their probability of interacting with LH waves. Recent studies have also indicated that the energy exchange between a particles and LH waves in reactor conditions could provide a mechanism for transferring LH wave energy to the plasma core [22]. This effect was not observed in the experiments performed in JET with ICRH fast minority ions.

VI–CONCLUSIONS

The first experimental evidence in JET on the interaction of fast minority ions with LH is reported in this work. An increase of approximately 20% in the fast ion energy content was observed in the presence of LH, with an estimated LH absorbed power of approximately 20% for 2MW of launched LH power and plasma densities of 2.0 to 2.4 x $10^{19} m^{-3}$ with central temperatures of $T_e(0) \sim 5$ to 8 keV. γ ray and neutron emission rates also show that absorption of LH waves by the fast minority ions is taking place. FFT analysis confirms a better damping of the wave when the overlap between ICRH and LHCD is maximised. Some other experiments performed in JT-60 and Tore Supra also confirm the predicted interaction between LH waves and non-thermal ions in the plasma and it has been observed that this interaction decreases when the wave frequency launched in the plasma increases. The choice of this frequency depends on the considered machine and on the dispersion relation of the wave in the plasma. The next JET operational campaign, where 10MW of LH are expected to be coupled to the plasma, will provide further information on the interaction between α particles and LH waves, as simulated with ICRH minority fast ions. This should allow an experimental assessment of the dependence on plasma parameters of the LH power damping on fast minority ions.

ACKNOWLEDGEMENTS

The theoretical background to this work was partly carried out by Dr. Barbato from ENEA (Frascati) under Article 14 with JET. We acknowledge useful

discussions with Dr. P. Froissard on the acquisition of FEB profiles, Dr. K. Lawson on the impurity analysis and discussions with Dr. F. Söldner. We acknowledge also the continuous encouragement of Dr. J. Jacquinot and the financial support given by the Brazilian National Research Council (CNPq), by the Commission of the European Communities and by JET Joint Undertaking.

REFERENCES

[1] C.F.F. Karney, N. Fisch, Phys. Fluids 22 (9), 1817 (1979).
[2] T.H. Stix, Waves in Plasma, AIP, New York, (1992).
[3] F.W. Perkins, Bull. Am. Phys. Soc. 27, 1101 (1982).
[4] N. Fisch, Rev. of Mod. Phys., Vol. 59, 175 (1987).
[5] E. Barbato, F. Santini, ITER-IL-PH-6-9-E-13 (1989).
[6] P. Pavlo et al., ITER - IL - PH-6-9-S-23 (1989).
[7] C.F.F. Karney, Phys. Fluids 22, 2188 (1978).
[8] M. Nemoto, et al., Phys. Rev. Letters, Vol. 67 No. 1, 70, (1991) Amsterdam, 3, 1183 (1990).
[9] C. Doloc, G. Martin, Proc. 20th EPS Conference, Lisbon, Part III, 895 (1993).
[10] M. Nemoto et al., Review of JT-60U Experimental Results from January to October, JT-60 Team, JAERI-M 93-057, 209 (1992).
[11] E. Barbato, Proc. 17th EPS Conference, Amsterdam, Part III, 1163 (1990).
[12] T.H. Stix, Nuclear Fusion 15, 737 (1975).
[13] G. Cottrell, D. Start, Nuclear Fusion, Vol. 31, 61 (1991).
[14] M. Brusati et al., Proc. Europhy. Top. Conf. on Radio Frequency Heating and Current Drive, Brussels, Belgium, 16E 225 (1992).
[15] D. Start et al., JET Report - JET-P(93)01, accepted for publication in Nuclear Fusion.
[16] L.G. Eriksson et al., JET Report - JET-P(93)01, accepted for publication in Nuclear Fusion.
[17] G. Sadler et al., Fusion Technology 18, 556 (1990).
[18] J. Jacquinot and the JET Team, Plasma Phys. Control. Fusion 35 A3 - A35 (1993).
[19] E. Righi et al., Proc. Europhy. Top. Conf. on Radio Frequency Heating and Current Drive, Brussels, Belgium, 16E 113 (1992).
[20] Y. Baranov et al., Proc. 20th EPS Conference, Lisbon, 3, 881 (1993).
[21] P. Froissard et al., Proc. 18th EPS Conference, Berlin, Part III, 389 (1991).
[22] N. Fisch, J.M. Rax, Phys. Rev. Letters 62, 612 (1992).

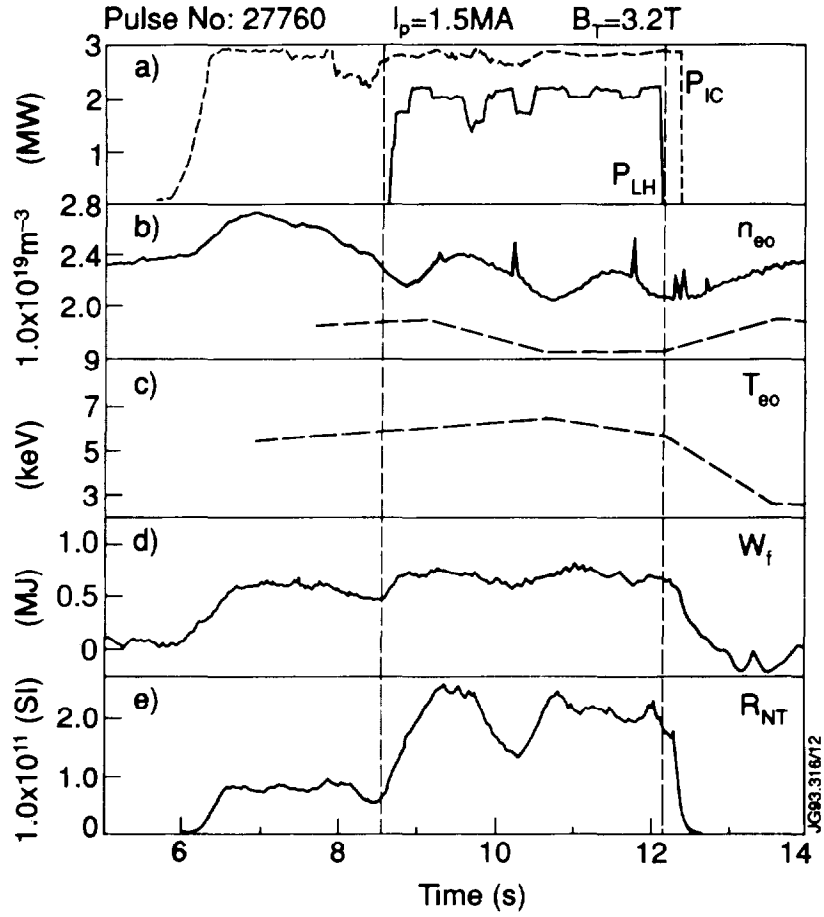

Fig. 1. Time evolution of the main plasma parameters, fast ion energy W_f and neutron rate for #27760. a) — LH power, --- ICRH power, b) — central electron density $n_e(0)$ (interferometer),--- $n_e(0)$ from LIDAR, c) --- central electron temperature $T_e(0)$ from LIDAR, d) increase on the fast ion energy (W_f) after 8.5s, e) neutron rate (RNT) showing an increase when LH is switched on.

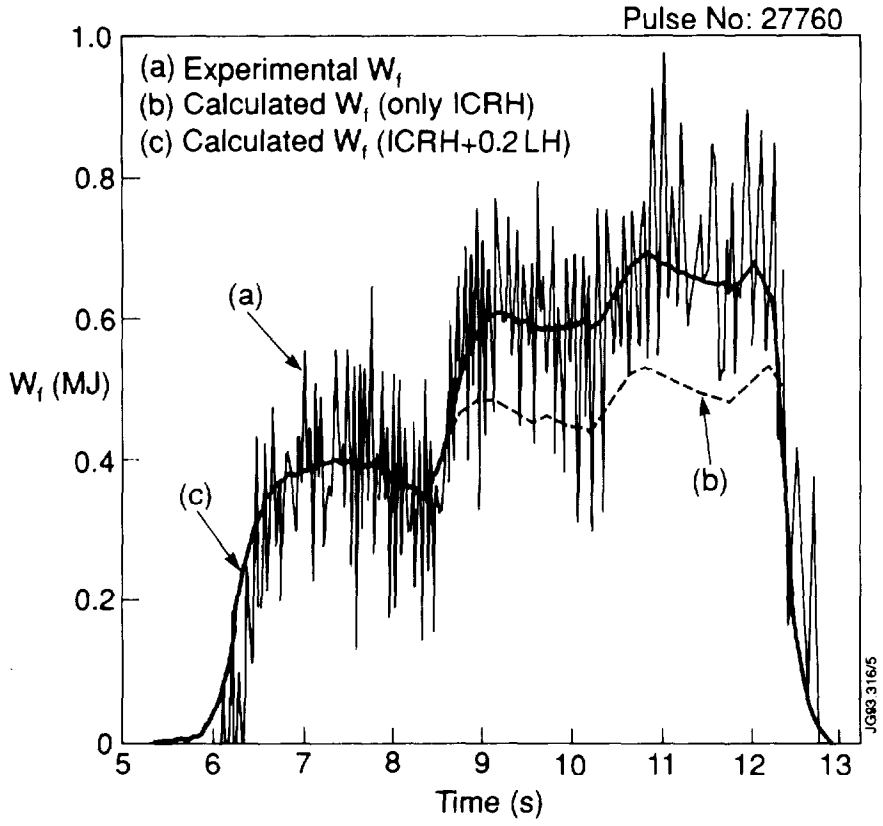

Fig. 2. Time dependent simulations show an increase of approximately 140kJ (18%) in W_f after 8.5s, due to LH. This corresponds to 20% of LH power damped on the fast minority ions.

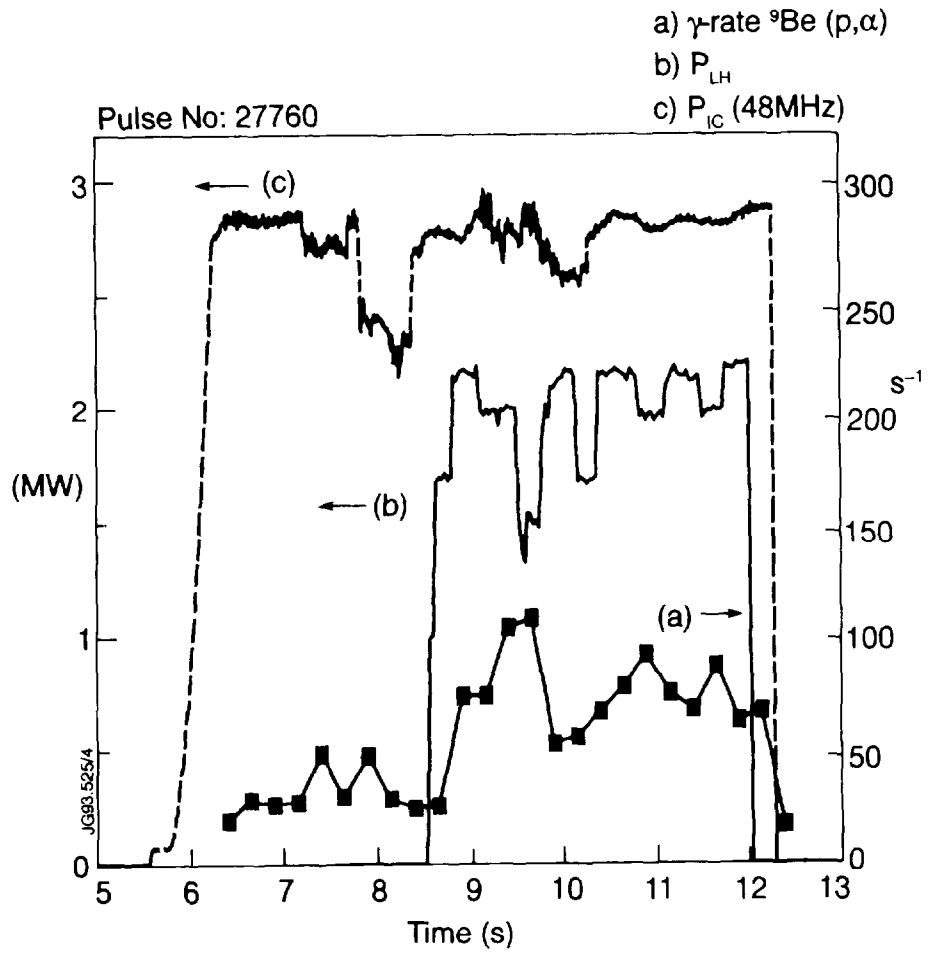

Fig. 3. (a) Gamma ray rate for #27760. An increase higher than a factor three is observed after LH (b) is launched in the plasma (8.5s). (c) ICRH power.

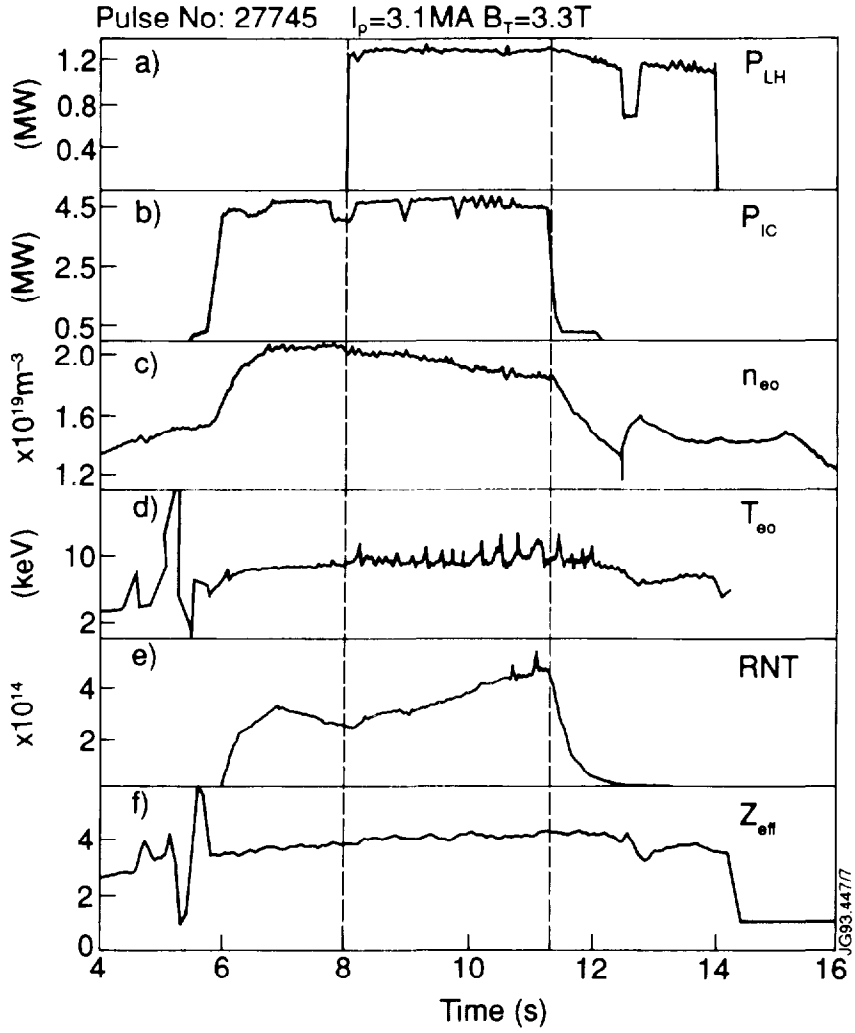

Fig. 4. Time evolution of the main plasma parameters and neutron rate for #27745. a) LH power, b) ICRH power, c) central electron density $n_e(0)$, d) central electron temperature $T_e(0)$, e) Neutron rate (RNT), f) effective charge Z_{eff}.

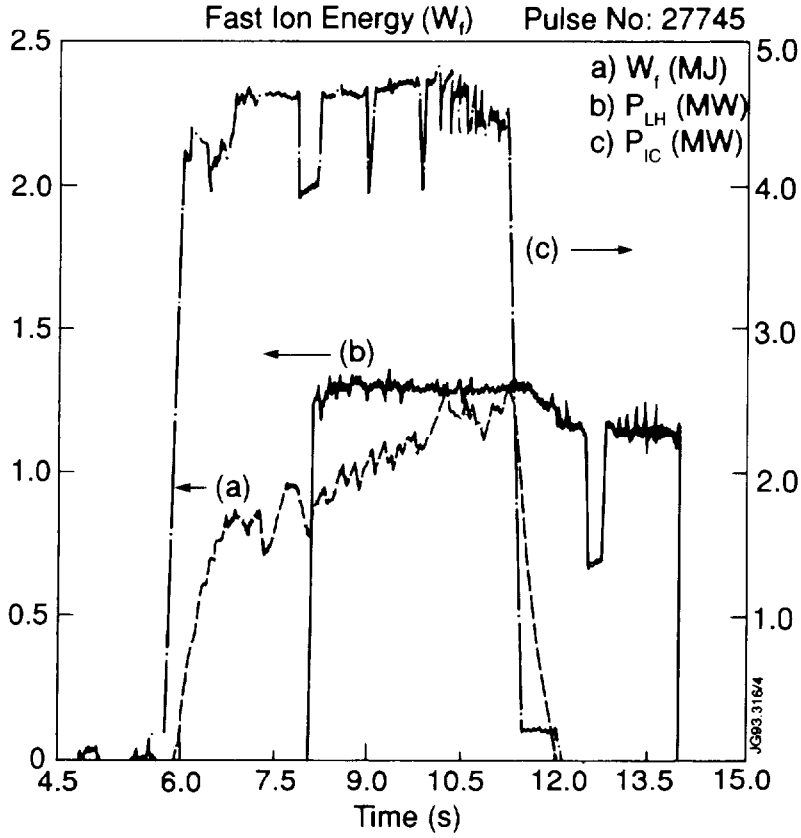

Fig. 5. Fast Ion Energy (W_f) increases monotonically when LH power is switched on. Curves b and c show the LH and ICRH power respectively for pulse #27745.

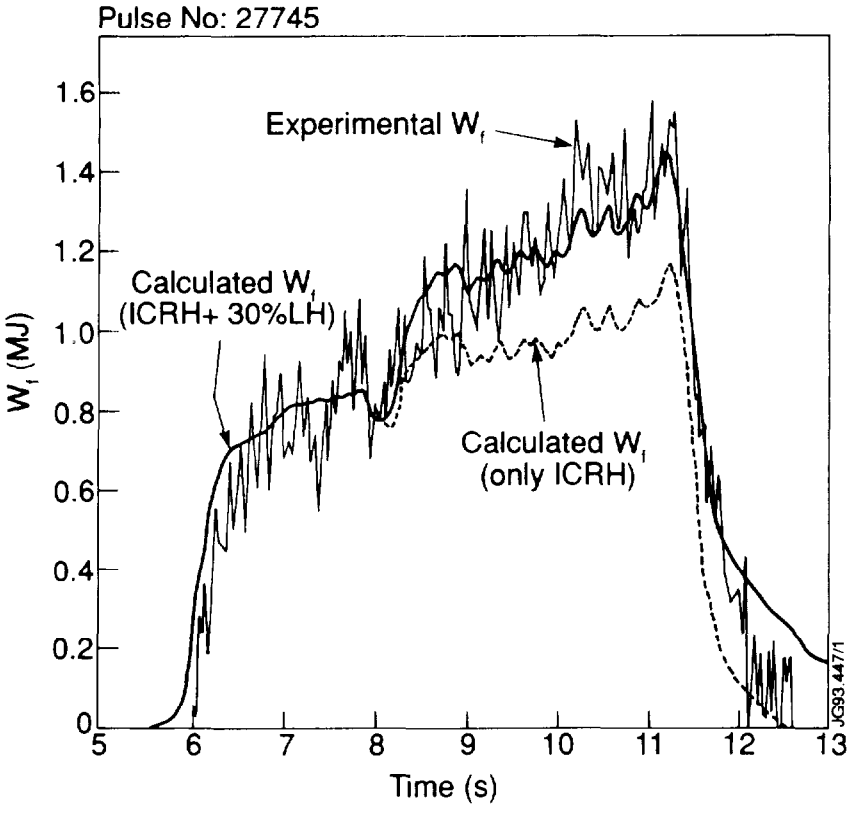

Fig. 6. Time dependent simulations of W_f for #27745 showing an increase of approximately 300kJ (22%) after 8.0s, due to LH. This corresponds to 30% of LH power damped on the fast minority ions.

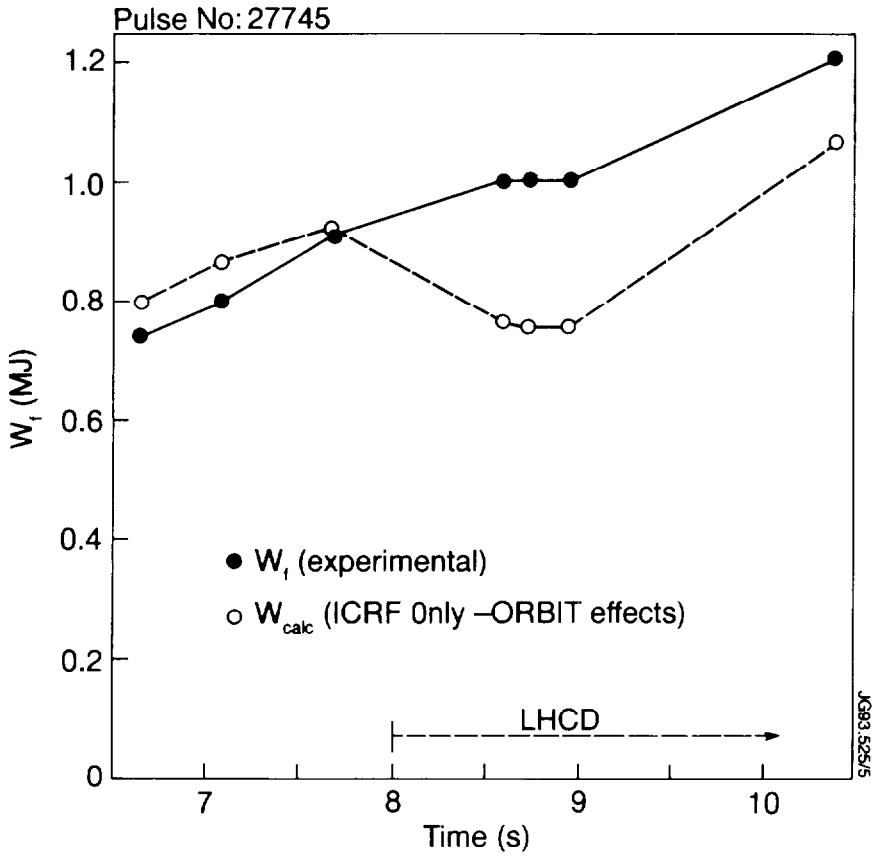

Fig. 7. Fast Ion Energy simulation including orbit effects for pulse #27745 taking into account ICRH power only. The agreement with the experimental data is good before LH is switched on (8s). After 8s the simulated values are lower than the experimental ones.

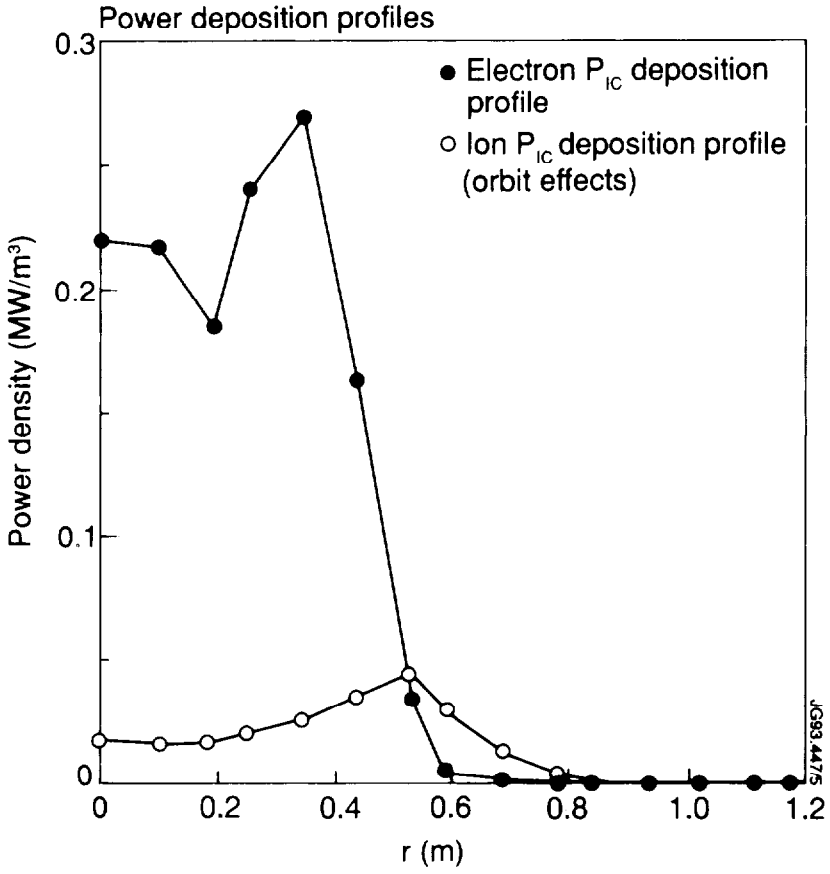

Fig. 8. ICRH power deposition on the electron (•) and ion (O) bulk populations taking into account orbit effects. The resonance layer is shifted to r ~ 0.35m and width of approximately 0.50m if a gaussian profile is taken into account.

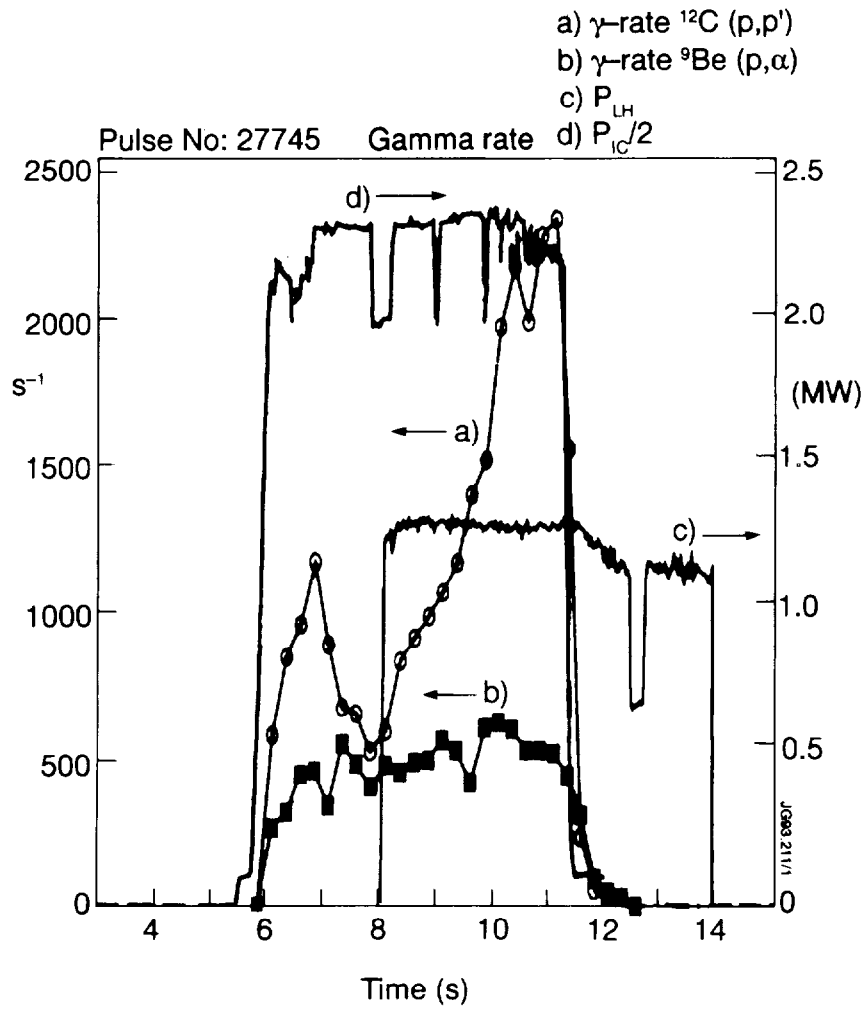

Fig. 9. Gamma ray rate for #27745. The 4.4MeV γ ray (a) increases substantially after 8.0s, showing an increase of the 5MeV ion population. b) γ ray at 3.5MeV. c) LH power. d) ICRH power.

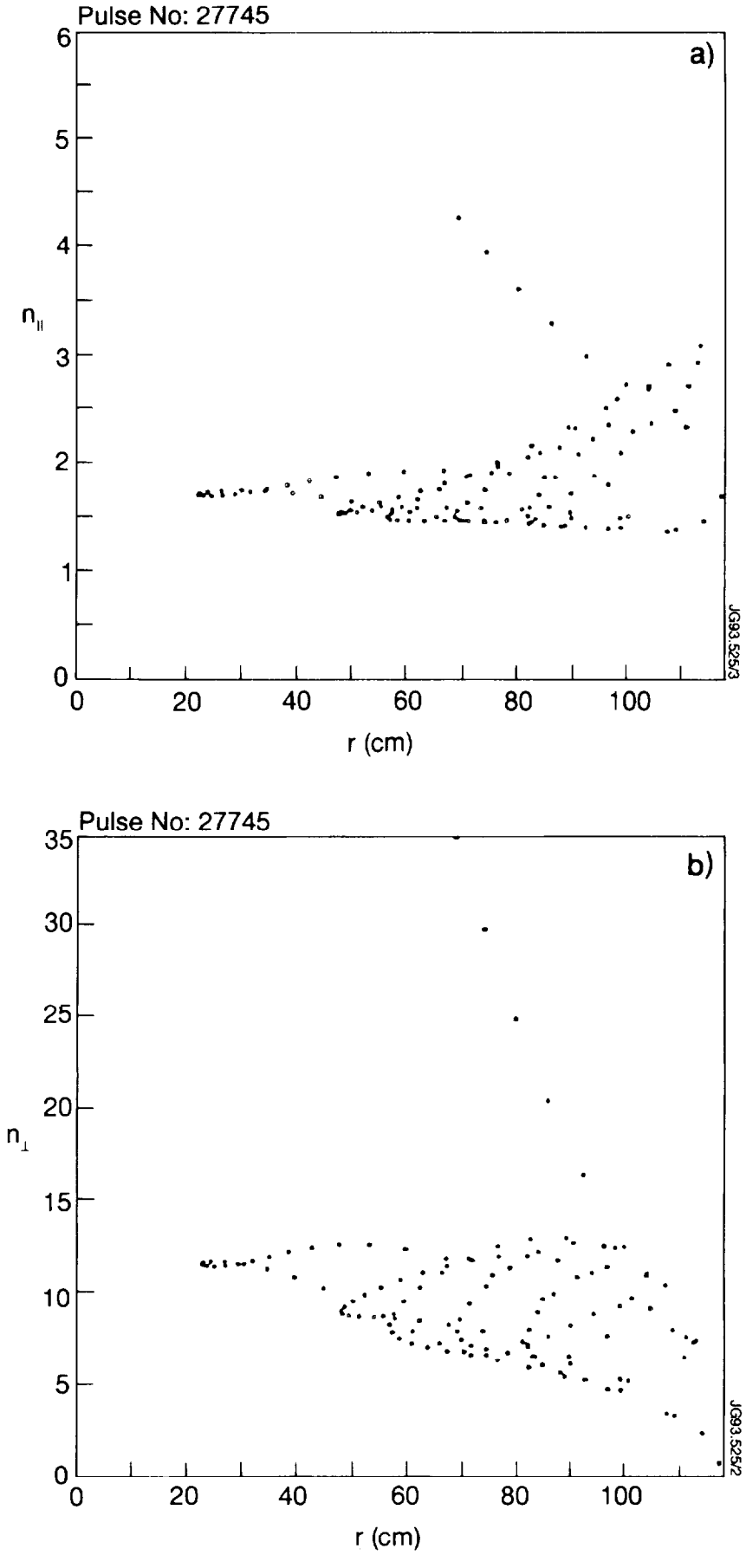

Fig. 10. Evolution of the wave refractive index from ray tracing calculation for #278745. a) $n_{\parallel}$ and b) $n_{\perp}$.

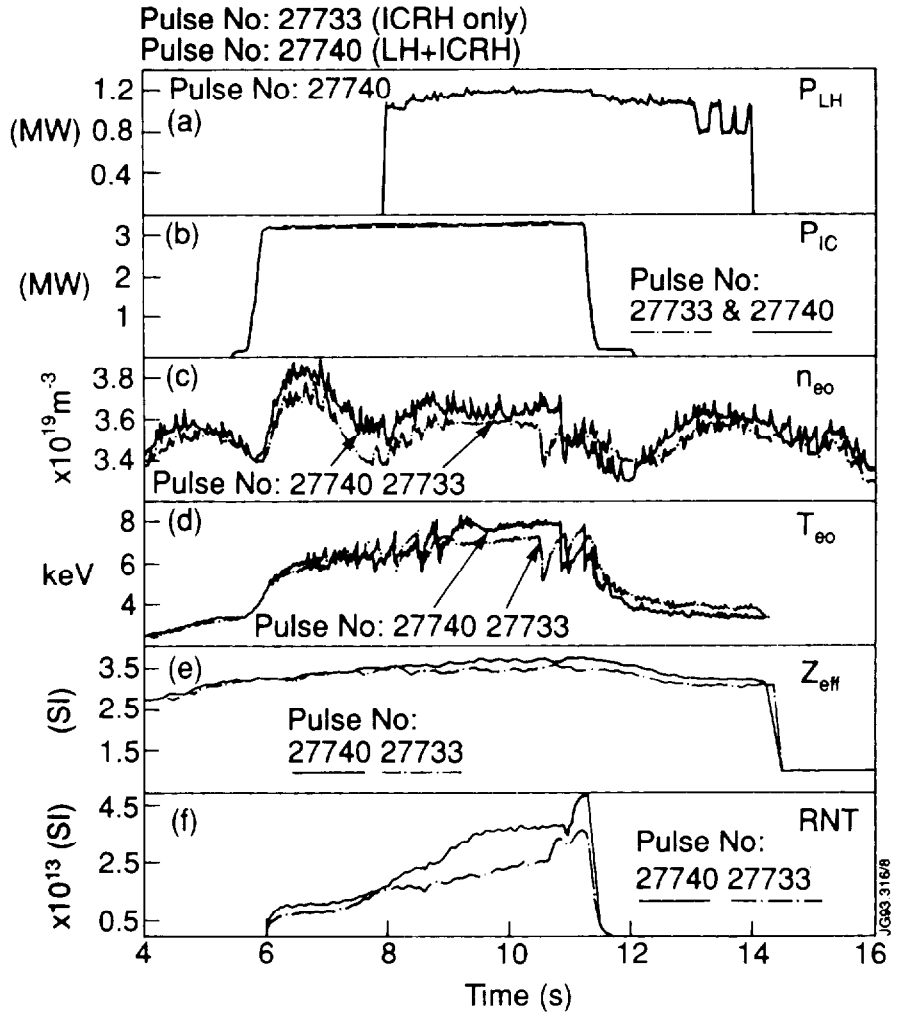

Fig. 11. Time evolution of the main plasma parameters and neutron rate for pulses #27733 and #27740. a) LH power, b) ICRH power, c) central electron density $n_e(0)$, d) central electron temperature $T_e(0)$, e) Z_{eff}, F) higher neutron rate showing an increase after LH is coupled to the plasma in #27740.

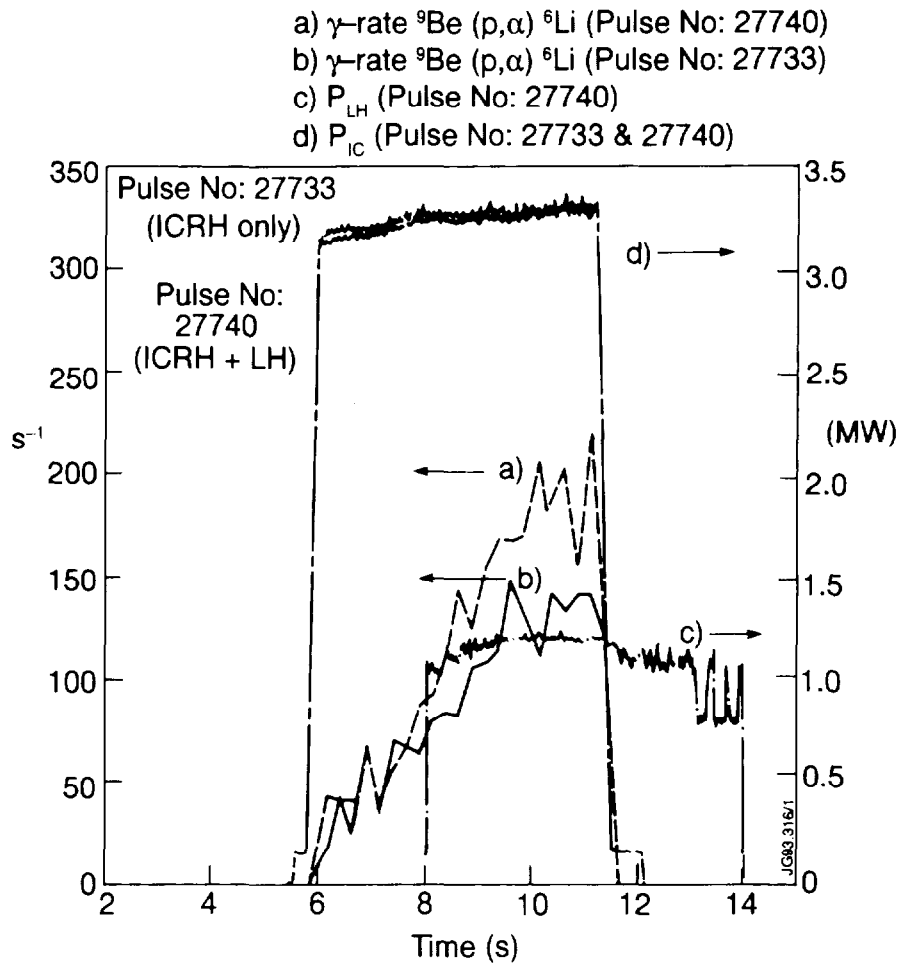

Fig. 12. Gamma ray count rate for pulses #27733 (b) (ICRH only) and #27740 (a) (LH + ICRH). c) LH power. d) ICRH power. There is a 30% higher increase on the γ ray rate for #27740 when LH is switched on.

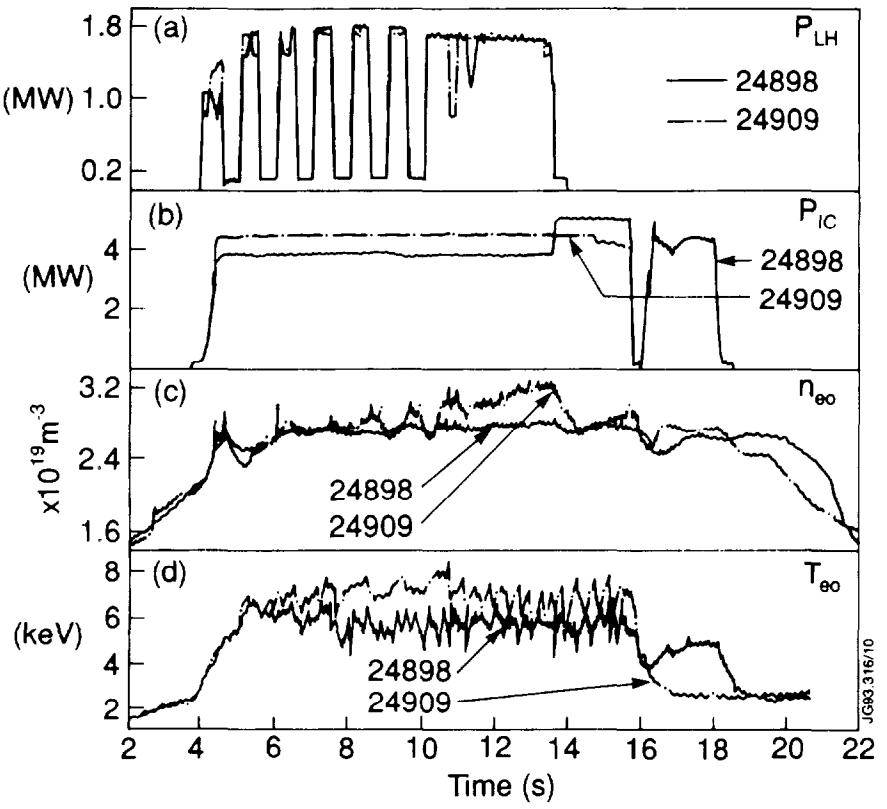

Fig. 13. Time evolution of the main plasma parameters for pulses #24898 and #24909. a) LH power, b) ICRH power, c) central electron density n_e (0), d) central electron temperature $T_e(0)$.

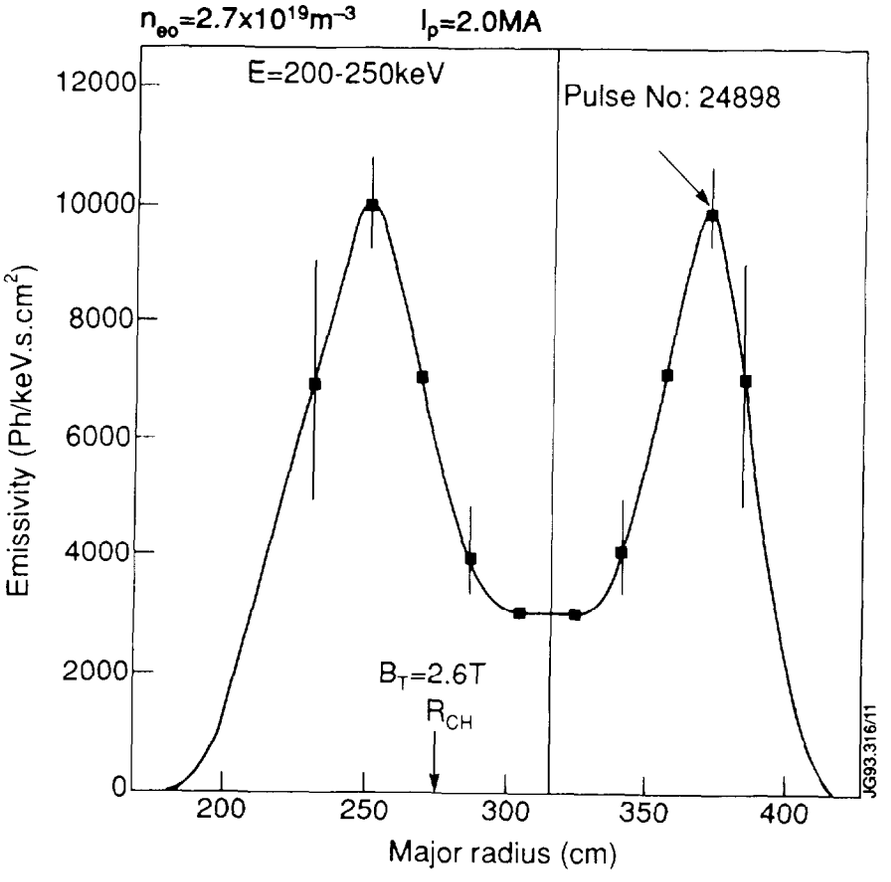

Fig. 14. Fast Electron Profile (FEB camera) for pulse #24898 peaked at r ~ 0.65 m close to the IC resonance layer, indicated at r ~ 0.40m.

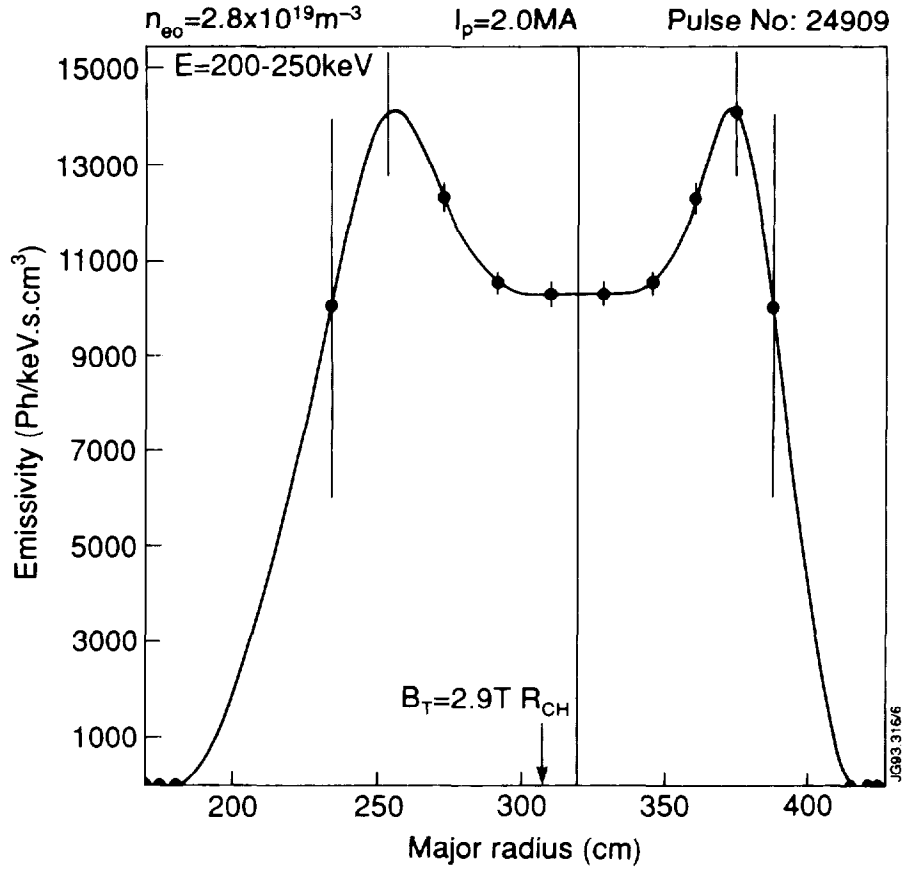

Fig. 15. Fast Electron Profile (FEB camera) for pulse #24909 peaked at r ~ 065 m. The IC resonance layer is indicated at r ~ 0.10 m.

a)

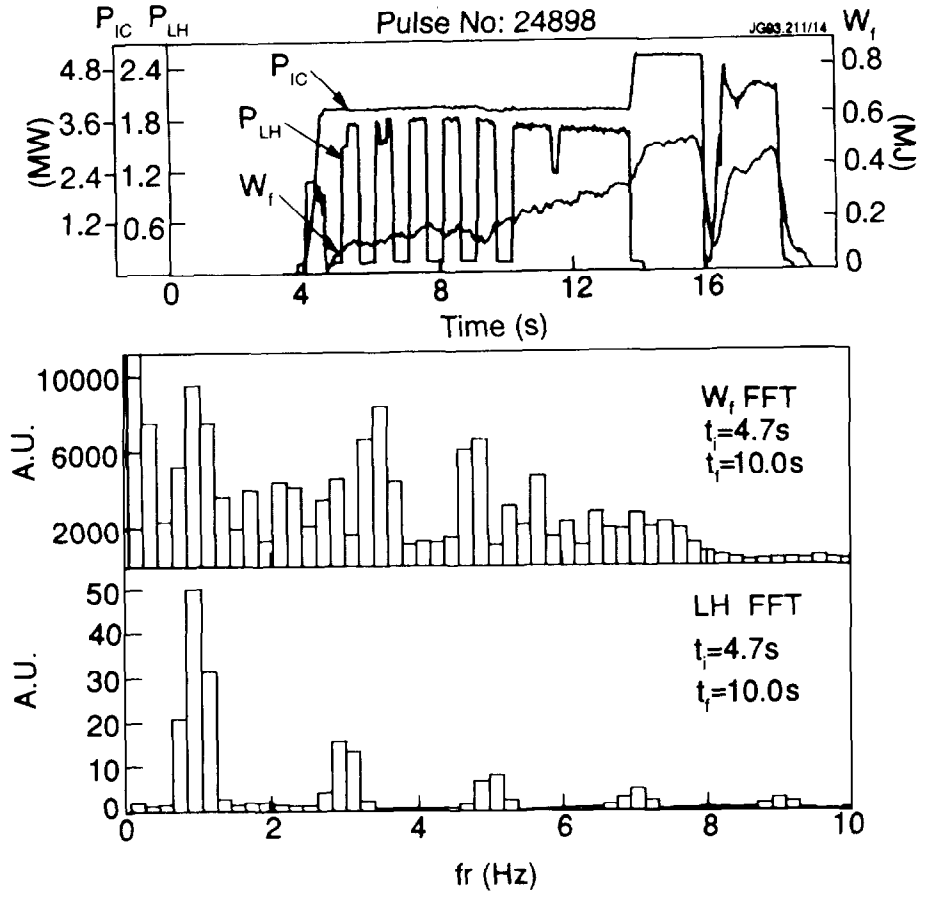
P_IC P_LH
Pulse No: 24898
JG93.211/14
W_f
P_IC
P_LH
W_f
(MW)
(MJ)
Time (s)
W_f FFT
t_i=4.7s
t_f=10.0s
LH FFT
t_i=4.7s
t_f=10.0s
A.U.
fr (Hz)

b)

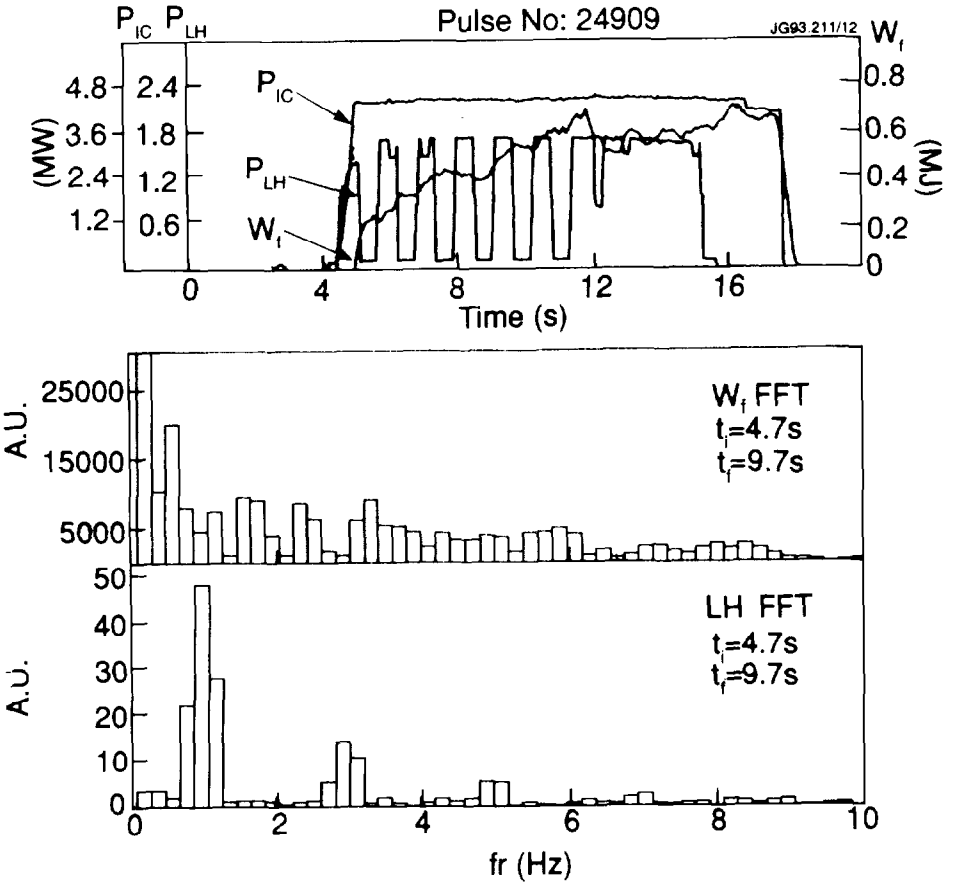
P_IC P_LH
Pulse No: 24909
JG93.211/12
W_f
P_IC
P_LH
W_f
(MW)
(MJ)
Time (s)
W_f FFT
t_i=4.7s
t_f=9.7s
LH FFT
t_i=4.7s
t_f=9.7s
A.U.
fr (Hz)

Fig. 16. Time evolution of fast ion energy and FFT analysis for W_f and LH for: a) #24898 (off axis) with $n_e(0) \sim 2.7 \times 10^{19} m^{-3}$ $B_T = 2.6T$ and b) #24909 (on axis) with $n_e(0) \sim 2.7 \times 10^{19} m^{-3}$ $B_T = 2.8T$. There is a peak on the W_f spectrum around 1 Hz, the frequency of LH power modulation, for #24898. Peaks in upper frequencies seem still to follow LH Fourier spectrum in this case. For #24909 the FFT on W_f does not show any evident peak at 1Hz, the frequency of LH power modulation.

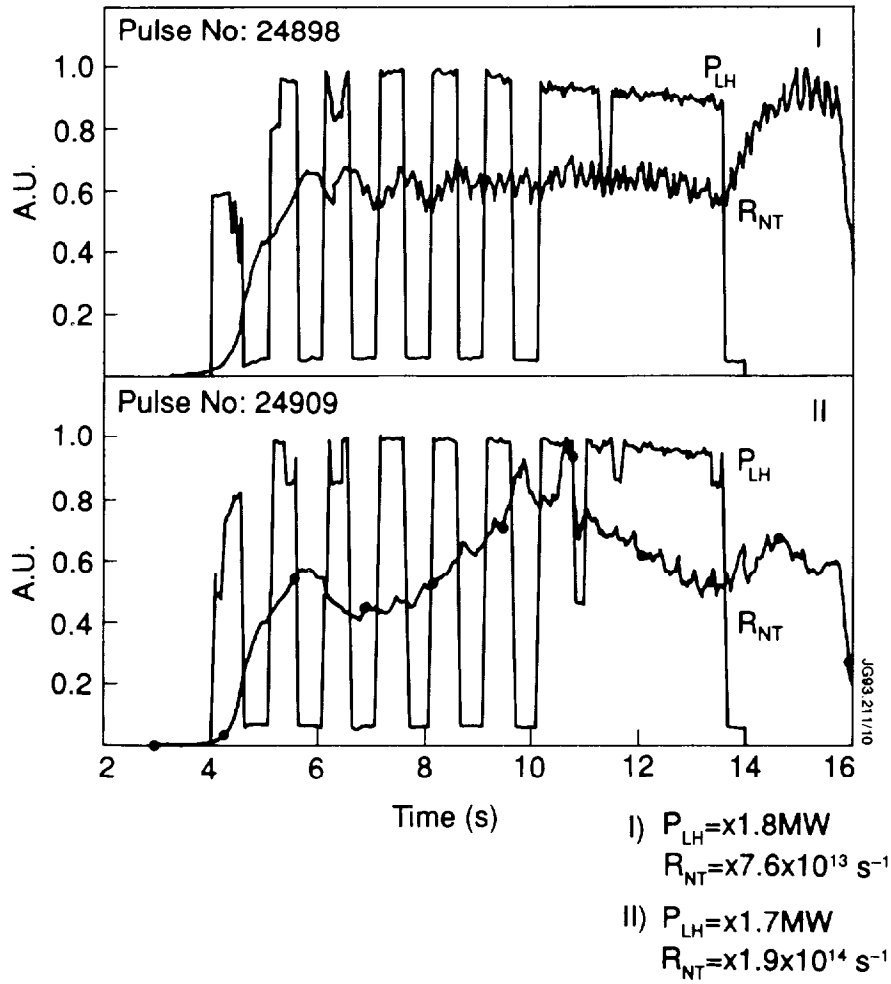

Fig. 17.Neutron Rate for pulses #24898 (I) and #24909 (II). It follows the LH modulation for #24898.

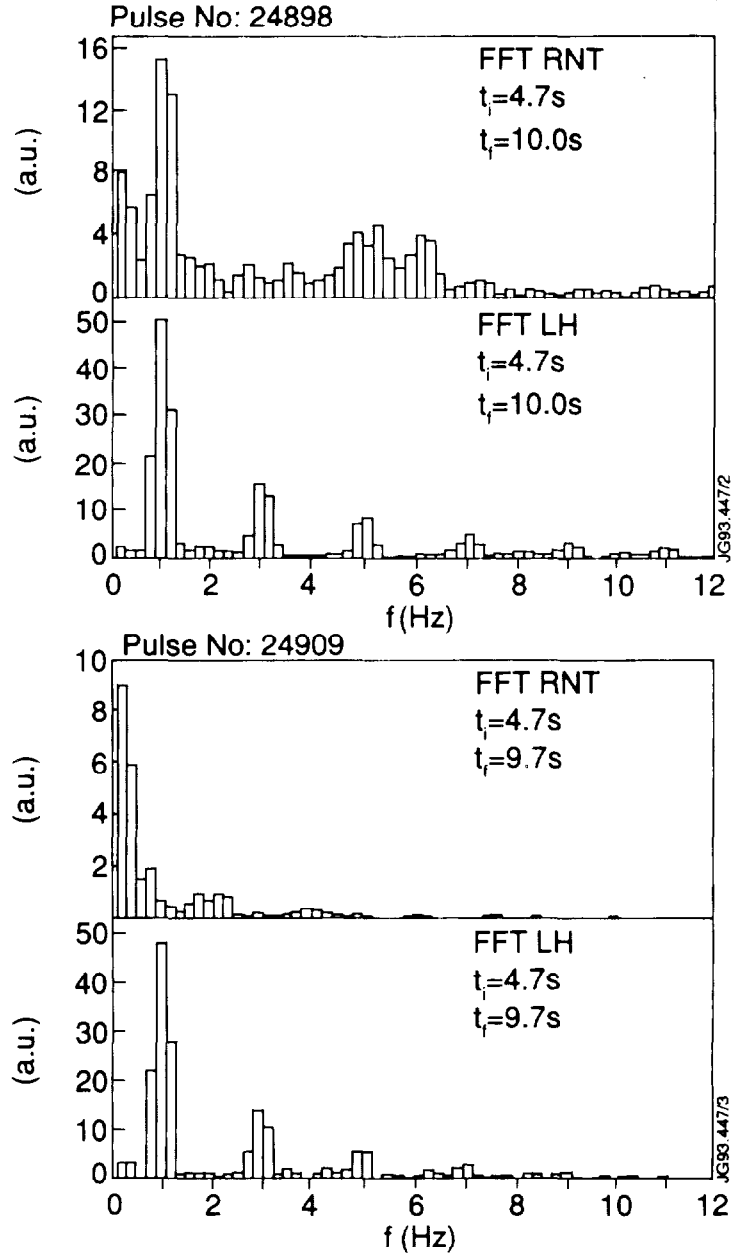

Fig. 18. FFT analysis for RNT and LH. a) #24898 (off axis). There is a clear peak on the RNT spectrum around 1Hz, the frequency of LH power modulation. b) #24909 (on axis). In this case the F FT on RNT does not show and peak at 1Hz.